# We are IntechOpen, the world's leading publisher of Open Access books Built by scientists, for scientists

6,900
Open access books available

186,000
International authors and editors

200M
Downloads

Our authors are among the

154
Countries delivered to

TOP 1%
most cited scientists

12.2%
Contributors from top 500 universities


WEB OF SCIENCE™

Selection of our books indexed in the Book Citation Index in Web of Science™ Core Collection (BKCI)

## Interested in publishing with us?
## Contact book.department@intechopen.com

Numbers displayed above are based on latest data collected.
For more information visit www.intechopen.com

Chapter 11

# Hydrogenation of Carbon Oxides on Catalysts Bearing Fe, Co, Ni, and Mn Nanoparticles

T.F. Sheshko and Yu. M. Serov

Additional information is available at the end of the chapter

http://dx.doi.org/10.5772/47743

## 1. Introduction

One way of obtaining synthetic liquid fuels and valuable chemical compounds on the basis of non-oil raw materials (coal, natural gas, biomass) is the synthesis of hydrocarbons from CO and $H_2$, which takes place with the participation of catalysts containing transition metals of Group VIII, known as the Fischer-Tropsch synthesis [1-3]. Although there are other methods for hydrocarbon mixtures of non-oil raw materials (for example, hydrogenation of coal and biomass pyrolysis and semi-coking coal), the priority development of the Fischer-Tropsch process clearly demonstrates its vitality and promise, as determined by an enormous source of raw materials - coal in the energy equivalent an order of magnitude higher than the oil.

In addition to carbon monoxide for the hydrogenation reaction is possible, and repeatedly described the synthesis of hydrocarbons from mixtures containing carbon dioxide [3-6] and hydrogen according to the equation of general form:

$$nCO_2 + (2n + m)\, H_2 \rightarrow CnH_{2m} + 2n\, H_2O$$

The use of carbon dioxide is one of the most promising directions of development of efficient catalytic systems that allow atmospheric pressure to convert the process emissions containing both CO and $CO_2$ in the olefins.

Global trend, most pronounced in industrialized countries, it became tougher environmental legislation. It is aimed primarily at reducing harmful emissions, which led to a sharp increase in the number of works connected with the search for technologies that could be returned to the commercialization of gas by-products. Process emissions include both mono-and carbon dioxide, and hydrogen. Develop and implement new and improved catalysts, allowing atmospheric pressure to convert these emissions into olefins is one of the

INTECH
open science | open minds

© 2012 Sheshko and Serov, licensee InTech. This is an open access chapter distributed under the terms of the Creative Commons Attribution License (http://creativecommons.org/licenses/by/3.0), which permits unrestricted use, distribution, and reproduction in any medium, provided the original work is properly cited.

most promising directions of development of nanotechnology and can make a significant contribution to solving the problem of reduction of pressure on the environment.

That is why the aim of this study was to investigate the possibility of obtaining olefins from a mixture of carbon oxides with hydrogen at atmospheric pressure, as well as determine the effect of the composition and characteristics of the catalysts containing transition metal nanoparticles on their activity and selectivity to olefins.

## 2. Experimental

### 2.1. The method of catalytic experiments

Catalytic activity in hydrogenation reactions of carbon dioxide, and mixtures of carbon oxides was determined by applying a mixture of genius with oxides of carbon and hydrogen in the ratio of the components [$CO_2$: $H_2$], [($CO_2$ + CO):$H_2$] = 1:2 and 1:4. Experiments were conducted in a flow catalytic apparatus at atmospheric pressure and flow rate 1.5 - 5.0 l/h, in the temperature range 423-723 K. The catalysts (weight 0.3-0.4 g) were placed in a quartz reactor with a quartz filter to prevent particle entrainment. Analyses of the products were performed chromatographically in a column of stainless steel filled with Porapack Q at 393K using a thermal conductivity detector and flame ionization. The rate of formation of reaction products W (mol/h*$g_{.at}$) was measured after reaching steady state and calculated per unit mass of metal (active) phase of the catalyst.

The catalysts were subjected to reduction treatment stream of hydrogen at a temperature of 623 K and flow rate of hydrogen 1.5-2.0 l/h before the catalytic.

### 2.2. The method of adsorption experiments.

The chemisorption of carbon oxides was investigated by thermodesorption. The adsorption of carbon oxides and hydrogen occurred when the reaction vessel was filled to atmospheric pressure with gases at temperatures of 293, 473, and 573 K. Thermodesorption was performed in a regime for a linearly programmed 293 to 823 K temperature increase in a helium flow. When needed, the products of thermal desorption from the reactor fed into nitrogen trap to remove water and carbon dioxide. The composition and amount of the desorbed gases were controlled using a Crystall 2000M chromatograph. All spectra of the thermoprogrammed desorption (TPD) were treated in terms of the coordinates of the Polyani–Wigner equation [7-10]:

$$-\frac{d\Theta_S}{dt} = \nu_n \Theta_S^n exp\left(-\frac{E_{a,des}}{RT}\right) \quad (1)$$

where $\theta_s$ is the surface coverage in terms of single layer fractions or the number of molecules adsorbed onto 1 $cm^2$ of the sample; $E_{des}$ is the activation energy of desorption; T is the temperature of the surface; n is the kinetic order of desorption; and $\nu_n$ is the frequency factor, $s^{-1}$.

To determine the activation energy of desorption according to the change in the surface concentration of an adsorbate during the thermodesorption process, the following integral equations for the first and the second order desorption were developed by Ehrlich [7,8]:

$$\frac{\ln\frac{\Theta_0}{\Theta_s}}{T^2} = \ln\frac{\nu_1 R}{\beta E_{des}} - \frac{E_{des}}{RT} \qquad \text{at } n = 1, \tag{2}$$

$$\frac{\ln\frac{\frac{1}{\Theta_s} - \frac{1}{\Theta_0}}{T^2}}{} = \ln\frac{\nu_2 R}{\beta E_{des}} - \frac{E_{des}}{RT} \qquad \text{at } n = 2, \tag{3}$$

where $\beta$ is the linear temperature rate of increase and $\theta_0$ is the maximum surface coverage that is proportional to the total area of the desorption peak. If the linear dependence were observed in presenting the experimental data in terms of Eq. (2) coordinates, the order of the desorption process would come first; if presented in terms of (3), the order would come second. It was according to this that the activation energy was found.

## 2.3. Methods of catalysts preparation.

Two series of catalysts were investigated. The first series was prepared matrixing in silicon oxide $SiO_2$ powders of iron and cobalt, which are obtained by electrochemical method[1]. We used high-purity silica particles which were the ultra-thin filament length of 1 mm and a diameter of 20-30 nm. The process of obtaining ultrathin crystals of metals occurs in a two-layer bath on the cathode surface, periodically or continuously wetted with a solution of the surfactant in an organic liquid. The lower layer is spun metal salt solution. The working surface of the cathode is located below the layer interface. Deposition of metal powder on the cathode is the formation of crystals, loosely connected with each other, between which there are gaps filled with an electrolyte solution, the metal oxides and hydroxides. By moving the cathode surface, or other mechanical action whiskers separated from the cathode and pass into the upper layer. Together with some of the top layer of liquid, powder extract from the electrolyzer and squeeze. This technology allows to obtain, depending on the electrolysis conditions whiskers of thickness 15-55 nm and lengths from 1 to several tens of micrometers.

The catalysts of the second series were obtained by plasma decomposition of a mixture of metals carbonyls vapors with hydrogen[2]. Hydrogen was the carrier and plasma gas. Couples metals carbonyls fed into the plasma-chemical reactor, the flow of hydrogen was bubbled through the liquid. Metal carbonyls decomposed in the plasma of a pulsed high-voltage capacitor, the frequency of 10 Hz, voltage pulses of 1 to 5 kW up to 100 microseconds. Speed of hardening produced ultrafine powders of metals reached $10^7$K/s. According to the data from transmission electron microscopy on an EMB100L instrument, the size of particles in the metallic phase was 2–25 nm on average. To synthesize bimetallic systems, nickel and

[1] The powders obtained by the Novocherkassk State University.

[2] The powders were obtained at the Moscow Academy of Steel and Alloys.

manganese were preliminarily deposited on aluminum oxide from aqueous solutions of their nitrates and exposed to a mixture of argon and oxygen at 623K. The aluminum oxide with the deposited metal was then placed in the plasma–chemical reactor, in which the iron and cobalt carbonyls were decomposed in hydrogen plasma. Templating the metallic particles into a supporter instantaneously during their formation prevents the separation of nanoparticles of the active phase from the supporter during the operation of the catalyst.

## 2.4. Methods of studying of physical and chemical properties of catalysts.

The catalysts surface layer was determined by X-ray photoelectron spectroscopy (XPS) at spectrometer XSAM-800 Kratos with a magnesium or aluminum anodes. The calibration of the spectra was carried out by C1s - carbon line (Eb = 285.0 eV). The pressure in the analyzer chamber was $10^{-9}$Pa. Identification of the elements was carried out by survey spectra. For quantitative analysis of surface composition using standard software processing and synthesis of the spectra.

The shapes and dimensions of particles in the powders were investigated by transmission electron microscopy (EMV-100L).

Specific surfaces of the powders were determined by low-temperature adsorption of nitrogen on the instrument GH-1 using the method of thermal desorption of nitrogen from the surface of solids. Constant composition gas mixture of nitrogen and helium was passed through the adsorbent at liquid nitrogen temperature prior to the establishment of adsorption equilibrium. Then, raising the temperature, nitrogen desorbed into a stream of gas mixture. Changing the concentration of the mixture at adsorption and desorption was recorded using thermal conductivity detector with programmable integrator ANALITIC-8C. The specific surface $S_s$ was calculated by the equation:

$$S_s = \frac{S_o V_m}{g} \tag{4}$$

where $V_m$ - gas volume that covers the surface of the adsorbent is a dense monolayer, $cm^3$; $S_0$ - surface covered with 1 $cm^3$ of adsorbate in a monomolecular layer, $m^2/m^3$; g-mass of adsorbent, grams.

Surface covered with a monomolecular layer of adsorbate is determined by the equation:

$$S_0 = \frac{N_A \sigma}{\tilde{V}} \tag{5}$$

Where $N_A$ - Avogadro's number; $\tilde{V}$ - volume of 1 mole of gas (cm3/mol); σ- the surface area of adsorbed gas molecules in a dense monolayer, for nitrogen σ = l, 62 * $10^{-18}m^2$.

$$S_0(N_2) = 4{,}35\ m^2/m^3$$

The value of Vm is determined by the equation of multilayer adsorption isotherm BET and counted in a special program integrator ANALITIC-8C.

The data on the composition and specific surface areas of the catalysts are given in Table1.

| Series | № | Catalysts | $S_{s.}$, $m^2/g$ |
|---|---|---|---|
| I | 1.1 | Fe(7.5%)-Co(2.5%)/$SiO_2$ | 4.0 |
| | 1.2 | Fe(6.5%)-Co(3.5%)/$SiO_2$ | 2.3 |
| | 1.3 | Fe(5%)-Co(5%)/$SiO_2$ | 1.3 |
| | 1.4 | Fe(2.5%)-Co(7.5%)/SiO2 | 1.0 |
| II | 2.1 | Ni(5%)/$Al_2O_3$ | 45 |
| | 2.2 | Fe(5%)/$Al_2O_3$ | 92 |
| | 2.3 | Co(5%)/$Al_2O_3$ | 25 |
| | 2.4 | Mn(5%)/$Al_2O_3$ | 20 |
| | 2.5 | Fe(5%)-Ni(5%)/$Al_2O_3$ | 65 |
| | 2.6 | Fe(5%)-Co(5%)/$Al_2O_3$ | 20 |
| | 2.7 | Fe(5%)-Mn(5%)/$Al_2O_3$ | 17 |
| | 2.8 | Fe(5%)-Co(2,5%)-Mn(2,5%)/$Al_2O_3$ | 18 |
| | 2.9 | Fe(5%)-Ni(2,5%)-Mn(2,5%)/$Al_2O_3$ | 63 |
| | 2.10 | Fe(5%)-Co(2,5%)-Ni(2,5%)/$Al_2O_3$ | 65 |

**Table 1.** The composition and specific surface areas of the catalysts.

## 3. Results and discussion

### 3.1. Physico-chemical properties of the catalysts

According to electron microscopy, the first series of samples (Table 1) of different particle shape. Each was a single crystal alloy with different percentages of iron and cobalt. Samples of catalysts № 1.1 and № 1.3 were a whiskers length from 0.1 to several micrometers and a diameter of 20 nm, the sample № 1.2 had a dendritic structure of intergrown crystals and particles of the sample № 1.4 were characterized by a hexagonal structure. Figure 1 shows a micrograph of crystals of iron, obtained by electrochemical method.


**Figure 1.** Micrograph of a iron micro-thin crystals, obtained by electrolysis (increase of 25000).

For the second series of samples it was found that powders contain both individual particles and their agglomerates. The particle size of the metallic phase averaged - 20 nm. Figure 2 shows a micrograph of a sample of iron powder. The smallest particle size of 2-5 nm is not facet and form large agglomerates that are difficult to beat at ultrasonic dispersion. The particles with sizes of 5-15 nm were weak faceting, while larger particles with sizes of 15-25 nm faceted clear.

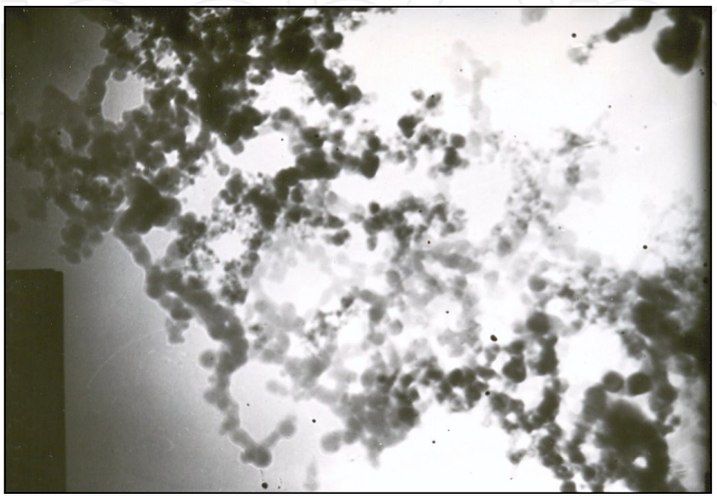

**Figure 2.** Micrograph of a iron sample obtained by plasma method (increase of 120000).

XRD ("Drone-7") and XPS were found in samples of the second series of catalysts (Table 1), $\alpha$-and $\gamma$-phases of iron, $\alpha$-and $\gamma$-phases of cobalt, $\alpha$-and $\beta$-phase nickel, small amounts of oxides, FeO, $Fe_3O_4$, $Fe_2O_3$, CoO, MnO, $Mn_2O_3$, $Mn_3O_4$, NiO, $Ni_2O_3$, solid solutions of $FeMn_3$, $FeMn_4$, as well as traces of $CoFe_2O_4$. Chemical analysis of these powders showed that they contained up to 3% of free and up to 2% fixed carbon, and about 80% of the metal.

### 3.2. The results of thermodesorption experiments and analysis.

The method of thermodesorption established the presence of molecular and dissociative adsorption of both carbon oxides. When the joint adsorption of carbon oxides competition between CO and $CO_2$ did not occur. Installed desorption forms, orders and activation energies of desorption are shown in Table 2.

Analysis of the experimental and literature data [10-13] allowed to interpret the desorption form as follows:

$\alpha$-CO - low-temperature linear ;
$\beta$-CO - high-bridging;
$\gamma$-CO - dissociative adsorption $CO_2 : CO_2 \rightarrow CO_{ads} + O_{ads}$;
$\alpha$- $CO_2$ - low-temperature molecular;
$\beta$-$CO_2$ - high-molecular or at $CO_{ads} + O_{Me} \rightarrow CO_2$;
$\gamma$-$CO_2$ - or molecular, or $CO \rightarrow C_{ads} + O_{ads}$ ; $CO_{ads} + O_{ads} \rightarrow CO_2$;
$\kappa$-$CO_2$ - carbonate-carboxylate complexes $n(CO+CO_2)/mMe$.

| $T_{des}$, K | | 293-353 | 353-423 | 423-473 | 473-503 | 573-623 | 623-673 | 673-723 | 773-823 |
|---|---|---|---|---|---|---|---|---|---|
| CO | | $\alpha$- $CO_2$ | $\alpha$-CO | $\beta$-$CO_2$, $\beta$-CO | - | - | - | - | - |
| n | | 1 | 1 | 2 | | | | | |
| $E_{a,des}$, kJ / mol | $Fe/Al_2O_3$ | 27 | 32 | 49 | | | | | |
| | $Ni/Al_2O_3$ | 36 | 35 | - | | | | | |
| | Fe-Co/ $Al_2O_3$ | - | 61 | 82 | | | | | |
| | Fe-Mn/ $Al_2O_3$ | - | - | 94,50 | | | | | |
| $CO_2$ | | $\alpha$- $CO_2$ | | $\beta$-CO | $\gamma$-$CO_2$ | $\kappa$-$CO_2$ | - | - | $\gamma$-CO |
| n | | | | 2 | 1 | 1<n<2 | | | 2 |
| $E_{des}$, kJ / mol | $Fe/Al_2O_3$ | - | | - | 41 | 52 | | | 121 |
| | $Ni/Al_2O_3$ | 36 | | 114 | - | 211 | | | - |
| | Fe-Co/ $Al_2O_3$ | | | 110 | 45 | 52 | | | |
| CO+$CO_2$ | | | $\alpha$-CO | $\beta$-$CO_2$, $\beta$-CO | $\gamma$-$CO_2$ , $\beta$-CO | $\kappa$-$CO_2$ | $\kappa$-$CO_2$ | $\beta$-CO, $\kappa$-$CO_2$ | $\gamma$-CO |
| n | | | 1 | 2, 1 | 1 | 2 | 2 | 1,1<n< 2 | 2 |
| $E_{des}$, kJ / mol | $Fe/Al_2O_3$ | | | 30, 25 | 46, 118 | 51 | 57 | 126 | 122 |
| | $Ni/Al_2O_3$ | | 43 | 82,148 | 118 | | 94 | | |
| | Fe-Co/ $Al_2O_3$ | | 60 | 85,112 | 45, 120 | | | | |

**Table 2.** Forms, orders (n), and desorption activation energies ($E_{a,des}$) for the $Fe/Al_2O_3$, $Ni/Al_2O_3$, Fe-Co/$Al_2O_3$ and Fe-Mn/ $Al_2O_3$ II Series catalysts after the adsorption of CO, $CO_2$, and a mixture of CO and $CO_2$ at 293 K

It should be noted that the degree of dissociation of CO increased in a series of Ni, Co, Fe, Mn, and pre-adsorption of hydrogen on the surface hardening is caused due Me-C and contributed to the dissociative chemisorption of carbon monoxide.

As shown previously [6,8], and we have reiterated, on the surface of metals, capable of dissolving hydrogen chemisorbed possible existence of two forms: one of which is associated with only one metal atom ($H_I$), and another - strongly-adsorbed ($H_{II}$) - with a few. Chromatographic analysis of the primary products of desorption revealed that the surface of the catalysts occurred removing the weakly bound hydrogen, probably in the form of $H_I$ and hydrocarbons ($CH_4$, $C_2H_4$, $C_3H_6$).

According to the works reported by Popova et al and Sokolova et al [13,14] on transition metals desorption of CO in the mode of programmed temperature increase leads to dissociation of the adsorbed gas on the carbon and oxygen and subsequent formation of a new form strongly-adsorbed CO desorption which occurs with higher activation energies.

When the temperature of desorption to the catalytic domain strongly adsorbed active carbon particles formed during the dissociative adsorption of CO on the catalyst surface begin to interact with hydrogen to form $H_{II}$ light hydrocarbons, which are allocated to the gas phase.

Pre-saturation of the iron-containing catalysts with hydrogen led to a change in the electron density of the catalyst surface, due to the introduction of hydrogen atoms in it. As a result, the TPD spectrum obtained after exposure of the catalyst with a mixture of CO and $CO_2$ (Figure 3), no peaks $T_{des}$ = 433K (CO formed by dissociative adsorption of $CO_2$) and $T_{des}$ = 523K ($\gamma$-$CO_2$), and the intensity the other peaks was lower than that of the similar peaks in the case of the initial sample. Similar results were obtained in experiments with a nickel catalyst (Figure 1).

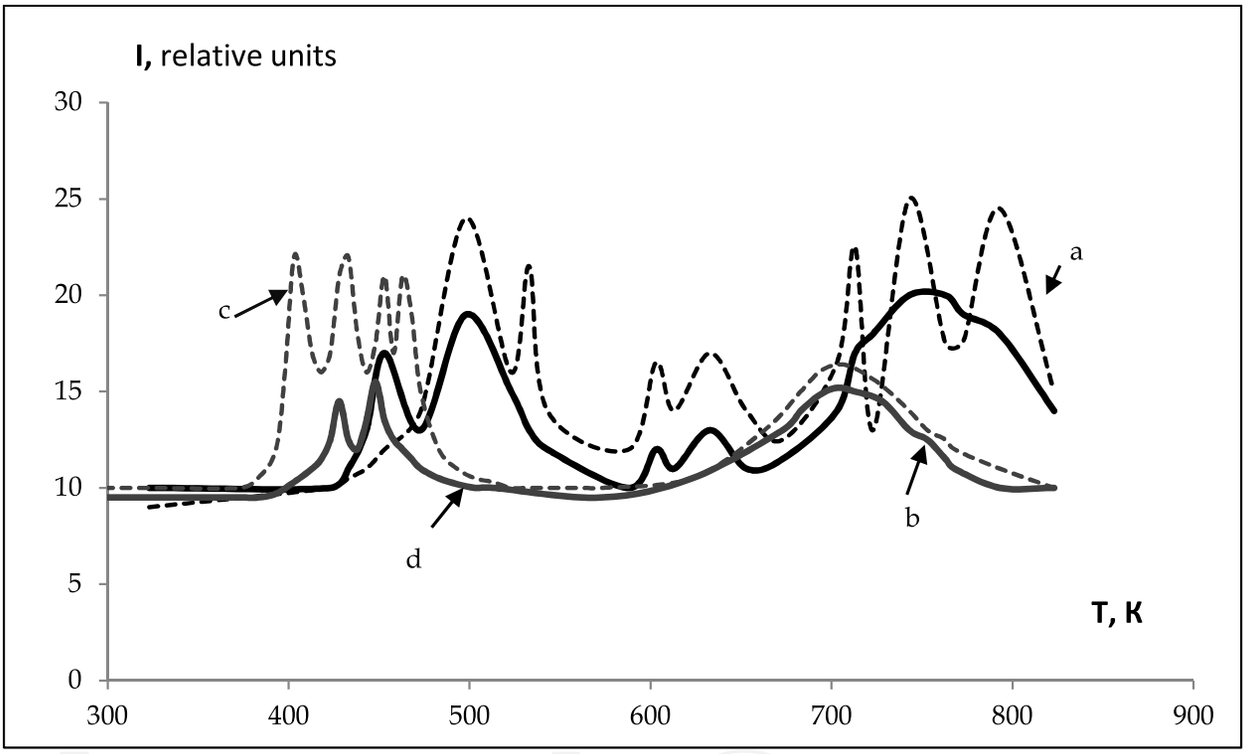


**Figure 3.** TPD spectra from the $Fe/Al_2O_3$ (a) and $Fe\text{-}H/Al_2O_3$ (b) , $Fe\text{-}Ni/Al_2O_3$(c) and $Fe\text{-}Ni\text{-}H/Al_2O_3$ (d) surfaces after coadsorption of CO and $CO_2$ at 293 K.

According to the works reported by Tananaev et al [15], in the presence of adsorbed hydrogen on the surface of ($H_I$) decreases the number of d-electrons of the metal involved in the formation of a bond M-C, with the result that the relationship is weakened and, therefore, communication is strengthened CO. Using a model two-dimensional electron gas is shown in [18] that modify the metal adsorption on the surface due to the redistribution of electron density ($n_e$) surface, and the partial diffusion of the adsorbate in the metal volume slightly reduces this effect. It can be assumed that the hydrogen $H_I$ is negatively charged and partially pulls the electrons in a metal. Its adsorption reduces the electron density, which leads to an increase in the number of weakly bound CO. It is known that dissolved in the metal hydrogen ($H_{II}$), on the contrary, very strongly protonated, and its electron becomes itinerant electrons of the metal, it is likely that hydrogen increases the electron density of the metal

surface and leads to an increase in temperature desorption peaks decrease in intensity of thermodesorption and increase in the desorption activation energy, as well as the disappearance of the products of desorption from the surface of weakly bound low-temperature form $\alpha$-$CO_2$, that is to modifying of the surface state of catalysts, and as a consequence, a qualitative change in the desorption of products). Chemisorbed hydrogen $H_I$ is probably a modifier that reduces the $n_e$ part of the free surface, and reduces both the total and induced CO adsorption. Since in our experiments, the temperature range lying below the Curie point, it is natural to assume that the hydrogen in the form of $H_I$ was negatively charged, which confirms the above, the effect of this form of hydrogen on the electron density $n_e$.

### 3.3. Catalytic properties of systems containing Fe, Co, Ni, and Mn nanoparticles.

Performing the reaction on the first series bimetallic catalysts (Table 1) at a ratio of the mixture [$CO_2$ : $H_2$] from 1:1 to 1:4 showed that the major reaction products were methane, ethane, ethylene, propane, propylene, carbon monoxide and water. Hydrogenation of carbon dioxide to methane (Fig. 4) becomes noticeable at 523-553 K and in all the samples of catalysts increases with increasing temperature. However, for samples № 1.2 and № 1.4 of the first series, which differ from the samples № 1.1 and № 1.3 the structure of metal particles at 613 K was observed at most. Further increase in temperature caused a drop in the rate of methane formation and the appearance of the products of carbon monoxide. Rate of formation of $C_2$-$C_4$ hydrocarbons for the first series of catalysts passes through a maximum, which is slightly shifted depending on the content of cobalt in the catalyst and the ratio of $CO_2$: $H_2$

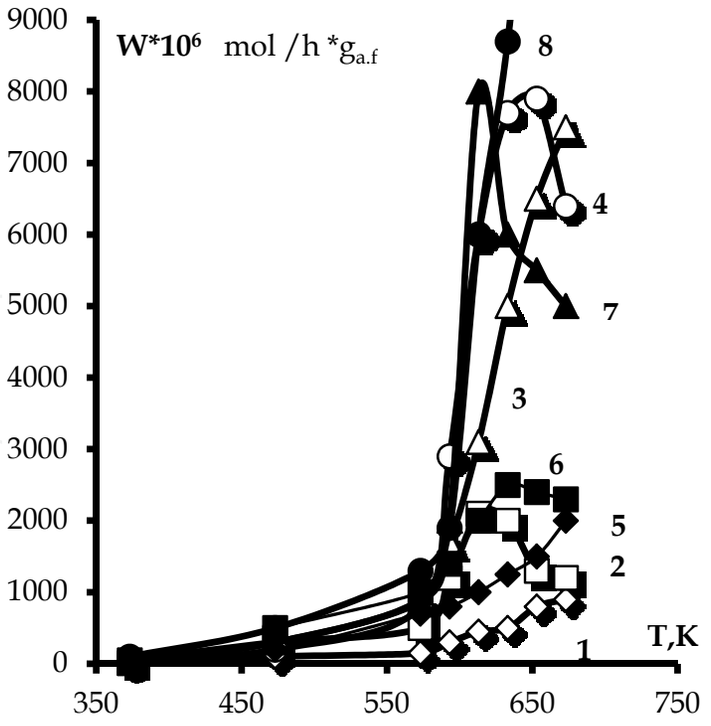


**Figure 4.** The temperature dependence of the rate of methane formation (W) on I group catalysts: with ratios of $CO_2$:$H_2$ = 1:1 in samples №1.1 (1), №1.2 (2), № 1.3 (3), № 1.4 (4); with ratios of $CO_2$: $H_2$ = 1: 4 to № 1.1 (5), №1.2 (6), № 1.3 (7), № 1.4 (8).

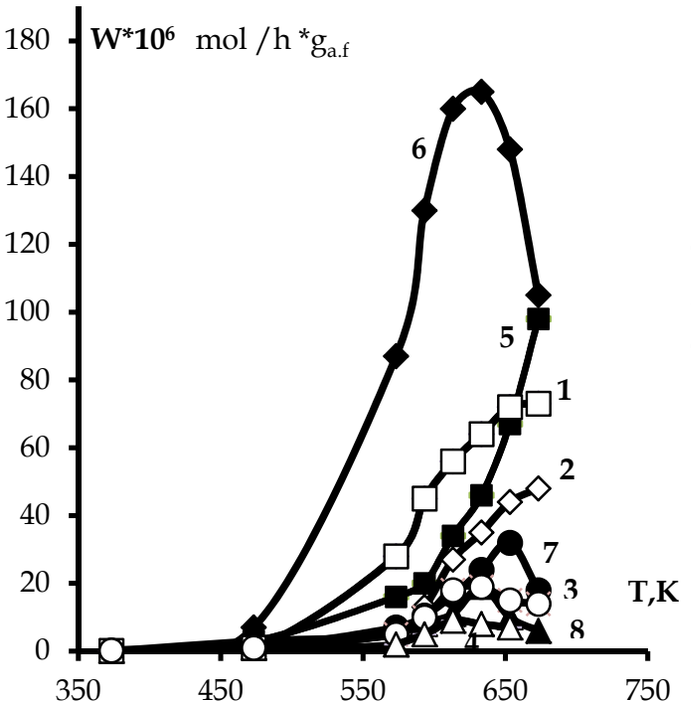


**Figure 5.** Dependence of the yields (W) of $C_2$-$C_3$ hydrocarbons on temperature on the sample №1.3 of the first series at a ratio of $CO_2$:$H_2$ = 1:1: $C_2H_4$ (1), $C_2H_6$ (2), $C_3H_6$ (3), $C_3H_8$ (4) at a ratio of $CO_2$: $H_2$ = 1:4 $C_2H_4$ (5), $C_2H_6$ (6), $C_3H_6$ (7), $C_3H_8$ (8).

The reaction to the lack of hydrogen ($CO_2$: $H_2$ = 1:1) increased the number of formed olefins and paraffins - declined. These patterns are shown in Fig. 5 for example, sample №3, containing equivalent amounts of iron and cobalt.

The total selectivity to olefins was highest for the № 2 catalyst and it was 30.2% at 573 K in the lack of hydrogen (Table 3). Increasing the hydrogen content in the mixture to 1:4 led to an increase in the number of produced hydrocarbons, but the drop in selectivity to olefins.

The increase in cobalt content in the catalyst led to an increase in the rate of formation of all products: as paraffins and olefins (Fig. 4, Table. 3). Probably, with increasing cobalt content in the single-crystal structure of iron-cobalt alloy is an increase in the number of active centers (growth $\ln k_o$). Changing the crystal structure of the catalysts (samples number 1.2 and number 1.4) leads to the creation of the crystals on the surface of larger number of high-active centers, which occurs at lower temperatures, dissociative adsorption of carbon dioxide with the formation of active carbon reacts with hydrogen [6, 15]. However, for sample №1.3 with the same content of both metals and having a thread-like crystal structure, a reduction in the rate of formation of olefins, probably due to the energy factor (Table 3). Since the specific surface area of the first group catalysts are similar, we can assume that their properties are determined only by the number of active centers and the crystal structure.

| series | № | Catalyst / $CO_2$:$H_2$= | $W_{CnH2n}$*$10^6$ mol /h *$g_{a.f}$ | | $S_{CnH2n}$, % | | Ea($_{CnH2n}$), kJ/mol | | $lnk_o$ | |
|---|---|---|---|---|---|---|---|---|---|---|
| | | | 1:1 | 1:4 | 1:1 | 1:4 | 1:1 | 1:4 | 1:1 | 1:4 |
| I | 1.1 | Fe(7.5%)-Co(2.5%)/$SiO_2$ | 2,50 | 5,90 | 10.3 | 4.6 | 27,6 | 32,3 | -5,9 | -5,1 |
| | 1.2 | Fe(6.5%)-Co(3.5%)/$SiO_2$ | 15,50 | 39,90 | 30.2 | 7.95 | 27,3 | 38,7 | -5,4 | -3,2 |
| | 1.3 | Fe(5%)-Co(5%)/$SiO_2$ | 84,00 | 29,90 | 20.9 | 2.8 | 60,0 | 44,2 | 1,9 | 1,1 |
| | 1.4 | Fe(2.5%)-Co(7.5%)/$SiO_2$ | 57,20 | 100,50 | 18.8 | 4.3 | 33,2 | 29,2 | -3,4 | -4,2 |
| II | 2.5 | Fe(5%)-Ni(5%)/$Al_2O_3$ | - | - | - | - | - | - | - | - |
| | 2.6 | Fe(5%)-Co(5%)/$Al_2O_3$ | - | - | - | - | - | - | - | - |
| | 2.7 | Fe(5%)-Mn(5%)/$Al_2O_3$ | 3,7 | 2,3 | 6,8 | 7,0 | 55,8 | 36,5 | -2,4 | 1,0 |

**Table 3.** The rate of formation, the total selectivity to olefins at 573K, the activation energy of formation of olefins and the logarithm of the pre-exponential factor.

It is known that the formation of olefins in the hydrogenation reaction of carbon dioxide at atmospheric pressure is not a characteristic of the deposited cobalt catalysts [4, 16-18] and on iron catalysts, the formation of olefins takes place at high pressures [4, 10]. However, the nanoparticles of the first group of samples have a large number of defects as a result of electrochemical synthesis, and for them there is practically no interaction between the metal carrier. This is likely to lead to the formation of active forms of carbon. Even more significantly, at atmospheric pressure and at any ratio of $CO_2$:$H_2$ highest selectivity to unsaturated hydrocarbons have been the catalysts with high iron content (Table 3). The increase in cobalt content causes an increase in the rates of formation of all products. The combination in a single crystal of the active phase of iron catalyst, which is responsible for the formation of olefins and cobalt, which has high catalytic activity, allowing to obtain a significant rate of formation of reaction products and high selectivity.

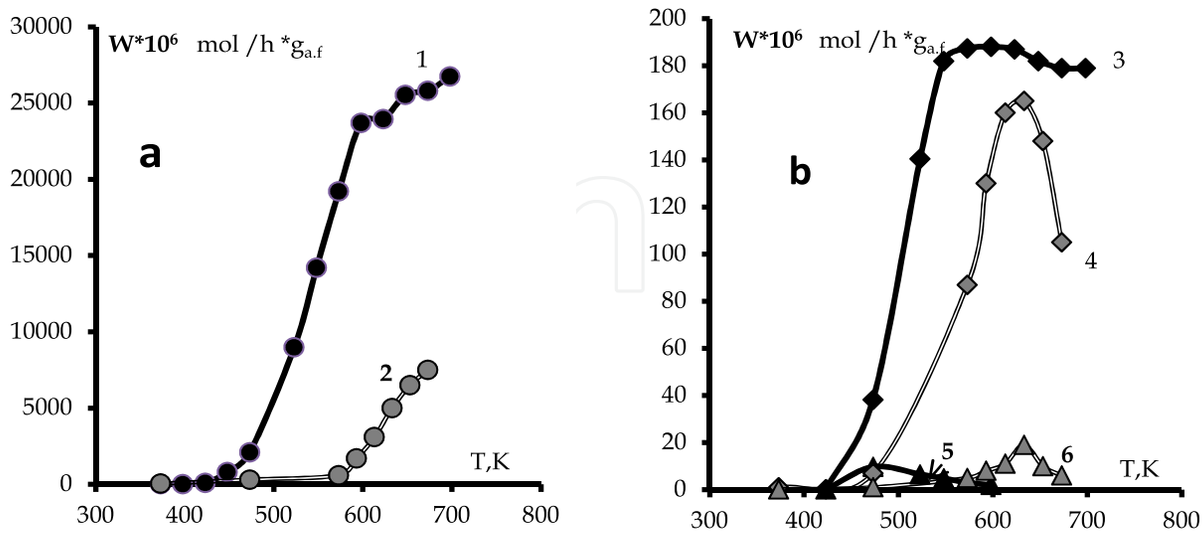


**Figure 6.** Dependence of the yields (W) of hydrocarbons on temperature when conducting the hydrogenation reaction with a $CO_2$ : $H_2$ ratio of 1 : 4: a) $CH_4$ on the catalyst № 2.6 Fe-Co/$Al_2O_3$ (1), on the catalyst №1.3 Fe-Co/$SiO_2$ (2); b) $C_2H_6$ (3, 4) and $C_3H_8$ (5,6) on the catalysts №2.6 Fe-Co/$Al_2O_3$(3,5) and № 1.3 Fe-Co/$SiO_2$(4,6).

Saturated hydrocarbons (methane, ethane and propane) were the main products during the hydrogenation of $CO_2$ to the sample №2.6 Fe-Co/$Al_2O_3$ of the II series catalysts under the same conditions and at the same ratios of reagents as for the samples of I group. The maximum amount of methane on the Fe-Co-sample was observed at 648K and was in 1489 * $10^{-6}$ mol /h *$g_{a.f}$, and a further increase in temperature resulted in the deactivation of the catalyst (Fig. 6).

Replacement of Co by Mn in the II Series catalysts resulted in the appearance of the reaction products of unsaturated compounds. Increasing the ratio of $CO_2$:$H_2$ to stoichiometric lead to an increase in both the rate of formation of olefins and selectivity for olefins (Table 4). It should be noted that the second series of samples with spherical particles of metal, templated in $Al_2O_3$, the number of generated hydrocarbons was higher than in the first series of samples with $SiO_2$ as carrier.

From the above data (Fig. 6, Table 3) that the catalytic activity of powders having a filamentary crystal structure (first series) is much lower than the activity of crystalline samples with an average particle diameter of 20 nm (second series). This may be due to the presence of point defects, dislocations, shear planes, edges and vertices of a crystalline metal catalysts of the second series, which leads to an increase in the number of active centers of the surface.

Introduction of CO in the reaction mixture $CO_2$:$H_2$ has increased the yield of olefins as ferromanganese, and the Fe-catalysts of II Series (Table 4). Quantitative characteristics of hydrogenation products were determined by the composition of the catalyst (Table 4). The highest yield of methane was observed when using Fe-Co/$Al_2O_3$. Substitution of cobalt for nickel or manganese resulted in a decrease in activity for methane formation in a series of Fe-Co/$Al_2O_3$ - Fe-Ni/ $Al_2O_3$ - Fe-Mn/ $Al_2O_3$.

Despite the low catalytic activity of ferromanganese catalyst for the formation of hydrocarbons, olefins selectivity on average 4-4.5 times higher than the figure obtained in the iron-cobalt and iron-nickel samples.

Comparison of the apparent activation energies of methane and ethylene, as well as the pre-exponential factor logarithm lnK0, indirectly characterizing the number of active centers of the surface, with data on activity and selectivity of Fe-Co, Fe-Ni and Fe-Mn binary systems nanopowder showed that differences in catalytic properties probably due to a different number and nature of the surface active sites, as well as the influence of the nature of the second component (Table 4). Thus, according to [3, 19-24], manganese primarily responsible for the formation of olefins and nickel and cobalt activate methane. This, apparently, explains the marked increase in selectivity to unsaturated products when replacing Co or Ni on Mn. At the same time Mn/ $Al_2O_3$ showed no catalytic activity for carbon oxides hydrogenation. However, the addition of Mn to Fe/ $Al_2O_3$ caused a significant increase in selectivity to olefins, in particular up to 50% at 573K.

Since Mn do not give olefins, this reaction is probably due to the fact that during the synthesis of the catalyst $Fe_xMn_y$ particles are formed. Moreover, Mn has a $\delta^+$ charge, since the ionization potentials of iron and manganese are different ($J_{Fe}$ = 7,893 eV, $J_{Mn}$ = 7,435 eV).

| № | 2.1 | 2.2 | 2.3 | 2.4 | 2.5 | 2.6 | 2.7 |
|---|---|---|---|---|---|---|---|
| | $Ni/Al_2O_3$ | $Fe/Al_2O_3$ | $Co/Al_2O_3$ | $Mn/Al_2O_3$ | $Fe-Ni/Al_2O_3$ | $Fe-Co/Al_2O_3$ | $Fe-Mn/Al_2O_3$ |
| $S_s$., $m^2/g$ | 45 | 92 | 25 | 20 | 65 | 20 | 17 |
| $W_{CH4}*10^6$ mol /h $*g_{a.f}$ | 241 | 80 | 9,2 | 0 | 243 | 808 | 20,8 |
| $W_{CnH2n}*10^6$ mol /h $*g_{a.f}$ | 0 | 12,2 | 0,5 | 0 | 14,3 | 138,8 | 24,7 |
| $S_{CnH2n}$, % | 0 | 11,8 | 5,1 | 0 | 5,6 | 14,0 | 54,3 |
| Ea($_{CH4}$), kJ/mol | 54,0 | 57,0 | | - | 86,8 | 65,2 | 58.3 |
| lnKo | 5,69 | 2,9 | | - | 9,38 | 6,42 | 3,46 |
| Ea($_{CnH2n}$), kJ/mol | - | 63 | | - | 64,6 | 48,9 | 31,7 |
| lnKo | - | 2,5 | | - | 5,2 | 1,32 | -4,0 |

**Table 4.** The yields of methane ($W_{CH4}$) and olefins ($W_{CnH2n}$), and the selectivity towards olefins ($S_{CnH2n}$, %) upon the hydrogenation of a mixture with the ratio [($CO_2$ + CO) : $H_2$] = 1 : 2 on II Series catalysts at 573 K.

The same effect was observed, but to a lesser extent $Fe-Ni/Al_2O_3$ and $Fe-Co/Al_2O_3$ (Table 4), which may also be associated with the occurrence of a positive charge on Ni and Co, but smaller than Mn, since the ionization potentials are close ($J_{Ni}$ = 7,635 eV, $J_{Co}$ = 7,87 eV).

Content analysis of the reactants in the gas phase at the joint hydrogenation of carbon oxides, showed that at room temperature, intensive adsorption as CO, $CO_2$ as the catalyst surface. The nature of the curves is identical for all samples studied and presented as an example $Fe-Co/Al_2O_3$ (Fig. 7) composition of the gas phase ($CO+CO_2$):$H_2$ has not changed

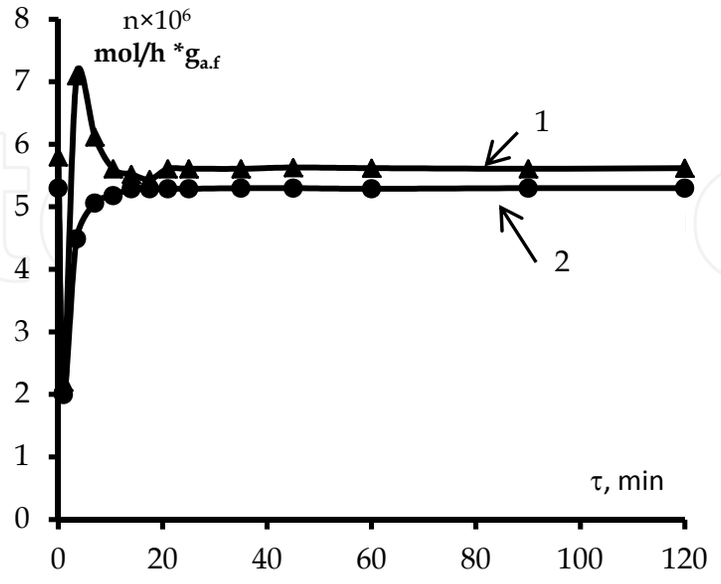


**Figure 7.** Amounts of CO (1) and $CO_2$ (2) in the gas phase during the adsorption on the catalyst № 2.6 $Fe-Co/Al_2O_3$

since the establishment of adsorption equilibrium and up to a temperature of 523 K. The transition temperature in the catalytic domain was accompanied by a decrease in the amount of CO and $CO_2$ formation (Fig. 8).

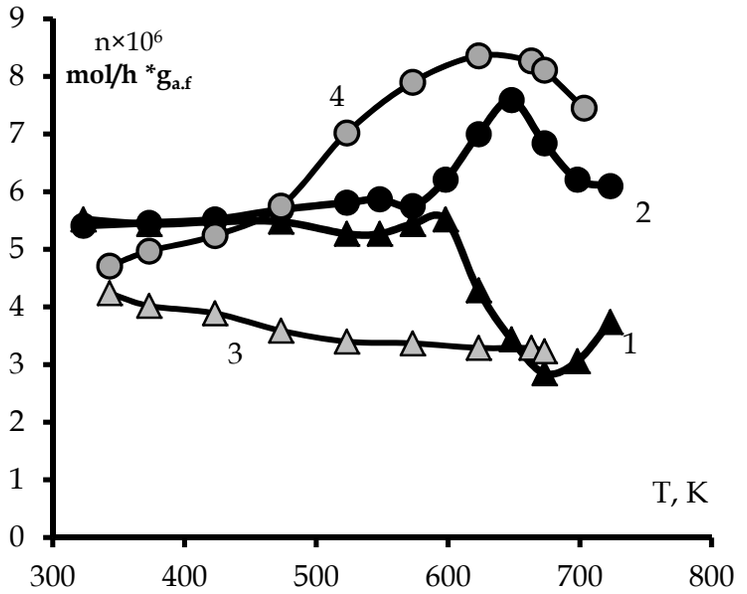


**Figure 8.** Amounts of carbon monoxide (1, 3) and dioxide (2, 4) in the gas phase during the hydrogenation reaction with a($CO+CO_2$): $H_2$ ratio of 1 : 4 on the catalysts № 2.6 Fe-Co /$Al_2O_3$ (1,2) and № 2.7 Fe-Mn/$Al_2O_3$ (3,4).

The formation of carbon dioxide is possible when an adsorbed oxygen atom released upon the dissociative adsorption of a CO molecule reacts with carbon monoxide adsorbed in the molecular form,

$$CO(ads.) + O(ads.) \rightarrow CO_2.$$

The probability of the occurrence of the disproportionation reaction of carbon monoxide:

$$2CO \rightarrow CO_2 + C$$

and of the reaction of steam conversion of CO:

$$CO + H_2O = CO_2 + 3H_2$$

is also high

These processes occur most intensively if the reaction is performed on an iron–manganese catalyst (Fig. 8). Replacing manganese with nickel results in a considerable reduction in the amount of formed $CO_2$ (Fig. 6), due possibly to the different quantities of the linear and bridged forms of adsorbed CO [25-27].

The trend of curves describing the temperature dependence of carbon monoxide concentration in a reaction mixture does not differ appreciably for reactions with a deficient or stoichiometric amount of hydrogen on the investigated catalysts, since it is possible that

only those carbon particles formed as a result of the dissociative adsorption of carbon oxides are involved in the reaction.

Thus, it is logical to assume that if the introduction of CO in the reaction mixture reduces the yields of saturated hydrocarbons and the resulting increase in the amounts of olefins, it is likely, during the flow process of adsorption of carbon oxides formed on the surface of carbon atoms with different catalytic activities: one - there are mostly in dissociative adsorption of CO and their interaction with surface hydrogen, leading to the formation of unsaturated hydrocarbons, and points arising from the chemisorption of $CO_2$ are responsible for the formation of both paraffins and olefins.

The ratio of saturated and unsaturated hydrocarbons in the hydrogenation products is determined basically by the amount of atomic hydrogen that is capable of migrating toward the surface's active centers, and by the structure of these centers [3, 6, 23]. As already mentioned, the adsorption of hydrogen on metals that are capable of dissolving it, the formation on the surface of the two forms of $H_2$ is possible [6]. One of them is weakly associated with only one metal atom ($H_I$), and another - strongly-adsorbed $H_{II}$ - with a few. CHx-radicals are formed from the active carbon, which is the product of dissociative adsorption of carbon oxides. However, the selectivity for olefins is probably determined by the ratio of forms $H_I$: $H_{II}$ on the catalyst surface and the increase in $H_I$ concentration of hydrogen increases the yield of olefins.

The chemical nature of the metal is also responsible for the appearance of some form of adsorbed substances. Among the iron-group metals, it is a linear complex of Co-CO, according to the works reported by Nieuwenhuys [28], the electron density at the carbon atom and the smallest such set is easier to interact with other chemisorbed particles. Therefore, of all the studied catalysts, regardless of how they receive the greatest activity was shown the iron-containing samples with the addition of cobalt.

In addition, the transition from bulk samples to nanoparticles and an increase in dispersion of the catalyst in its distribution on the supporter increases the coordinative unsaturation of metal atoms [29]. As a consequence, the binding energy of the metal varies not only with carbon but also a redistribution of hydrogen and the ratio $H_I$: $H_{II}$ regions in favor of the weakly bound hydrogen. This gives rise to additional forms of adsorption of carbon dioxide and an increase in selectivity to olefins.

Differences in the catalytic activity of the bimetallic samples could be associated with different rates of the diffusion of weakly bound hydrogen ($H_I$) on the catalyst surface through the contact boundaries between the Fe, Co, and Mn particles (a spillover effect), or with the existence of a jumpover effect [2, 3, 6, 11, 16]when $CH_X$ radicals formed in one centers carry centers from one gas phase to another, where their further hydrogenation by atomic hydrogen ($H_I$) to methane takes place. And the co-interaction of these $CH_X$ radicals leads to the formation as paraffins and olefins. The high selectivity to olefins ferromanganese catalyst may be due to the almost complete absence on the manganese surface of adsorbed hydrogen [9,12, 16]. And it contributes to the interaction between a $CH_X$-radicals.

To confirm this assumption, the idea [30,31] of the layered filling of the reactor has been used. The reaction mixture initially came to the catalyst layer of the iron nanoparticles templating in $ZrO_2$, and then held an insulating layer of $SiO_2$, and came on a layer of manganese in the $SiO_2$. The composition of products at the reactor outlet cardinally changed over the composition of products obtained by using only Fe / $ZrO_2$: significantly reduced the amount of methane, propane and butanes, and many times has increased the amount of olefins (Table 5).

| Catalyst | T,K | $W_{CH_4}$ | $W_{C_2H_4}$ | $W_{C_3H_8}$ | $W_{C_3H_6}$ | $W_{C_4H_8}$ | $S_{C_nH_{2n}}$ |
|---|---|---|---|---|---|---|---|
| Fe/$ZrO_2$ | 573 | 130,1 | - | 25,1 | 25,6 | 7,0 | 18,0 |
| | 623 | 869,1 | - | 118,0 | 169,0 | 29,3 | 16,7 |
| | 673 | 2084 | - | 348,0 | 511,0 | 69,0 | 19,2 |
| Mn/$SiO_2$ | 573 | 10,3 | - | 0,10 | 0,60 | 0,03 | 10,5 |
| | 623 | 13,5 | - | 0,24 | 0,90 | 0,04 | 6,4 |
| | 673 | 16,7 | - | 3,80 | 0,40 | 0,05 | 2,1 |
| Fe/$ZrO_2$+ Mn/$SiO_2$ | 573 | 33,0 | 1,0 | 9,0 | 70,0 | 52,0 | 73,0 |
| | 623 | 110,0 | 4,0 | 13,0 | 108,0 | 68,0 | 50,4 |
| | 673 | 230,0 | 2,0 | 18,0 | 134,0 | 82,0 | 46,7 |

**Table 5.** The yields (W*$10^6$mol /h *$g_{a.f}$) .) and the selectivity (S,%) towards olefins upon the hydrogenation of CO with the ratio CO : $H_2$ = 1 : 2 at atmospheric pressure.

The results confirm the suggestion that the iron generates CHx-radicals, which then transferred through the gas phase to the surface of manganese. It is their further recombination, mainly to olefins.

In carrying out the hydrogenation in the № 2.8 Fe-Co-Mn/$Al_2O_3$ and № 2.9 Fe-Ni-Mn/$Al_2O_3$ catalysts of the reaction products other than methane were also detected ethylene, ethane and propylene. At a stoichiometric ratio of carbon oxides and hydrogen, methane yields on these samples did not differ, but in an hydrogen's excess, a sharp increase in the amount of methane produced by Fe-Ni-Mn/$Al_2O_3$ than Fe-Co-Mn/$Al_2O_3$ (Table 6). Analysis of the rates of formation of other products showed that the catalyst containing nickel dominated saturated hydrocarbons, whereas on the Fe-Co-Mn sample was higher than the selectivity to unsaturated (Table 6).

The study of reactions on catalysts № 2.8 Fe-Co-Mn/$Al_2O_3$ and № 2.9 Fe-Ni-Mn/$Al_2O_3$ also identified a number of deviations from the above described processes. First, there was an increase in the apparent activation energy of formation of reaction products during the hydrogenation of an excess of hydrogen, in contrast to the bi-metal and Fe-Co-Ni system №2.10, where the trend is discernible only with respect to olefins, and for the saturated hydrocarbons were characterized, on the contrary, it decline. Secondly, the increase of

hydrogen content in the reaction mixture, or virtually no effect on the selectivity, or even lead to its growth in olefins and some reduction in methane (Table 6), whereas for the catalysts described above, the nature of these relationships were reversed.

| № | Catalyst | $S_{CH4}$, % | $S_{CnH2n}$, % | $Ea_{(CH4)}$, kJ/mol | $Ea_{(CnH2n)}$, kJ/mol |
|---|---|---|---|---|---|
| [$(CO_2 + CO) : H_2$] = 1 : 2 | | | | | |
| 2.8 | Fe-Co-Mn/$Al_2O_3$ | 62,9 | 26,2 | 90,6 | 56,2 |
| 2.9 | Fe-Ni-Mn/$Al_2O_3$ | 83,6 | 9,6 | 96,1 | 55,2 |
| 2.10 | Fe-Co-Ni/$Al_2O_3$ | 81,8 | 0,0 | 95,1 | 52,1 |
| [$(CO_2 + CO) : H_2$] = 1 : 2 | | | | | |
| 2.8 | Fe-Co-Mn/$Al_2O_3$ | 62,1 | 31,1 | 95,3 | 59,1 |
| 2.9 | Fe-Ni-Mn/$Al_2O_3$ | 83,3 | 11,0 | 106,2 | 81,9 |
| 2.10 | Fe-Co-Ni/$Al_2O_3$ | 95,3 | 0,7 | 90,9 | 30,4 |

**Table 6.** The selectivity towards methane ($S_{CH4}$) and olefins ($S_{CnH2n}$, % ) upon the carbon oxides hydrogenation on II Series catalysts at 573 K.

These data may indicate the formation under the influence of reaction medium on the surface of these polymetallic manganese catalyst of new centers responsible for the formation of olefins and requires more energy expenditure.

## 4. Conclusion

In the synthesis of hydrocarbons involved the active carbon formed by dissociative adsorption of carbon oxides on the catalyst surface. The differences in catalytic activity and selectivity of bimetallic samples are due, probably, different rates of the weakly bound hydrogen spillover ($H_I$), as well as speed $CH_X$ - radicals jump-over effect from one center to another, where they undergo further hydrogenation. The increase in dispersion of the catalyst can lead to a redistribution of the ratio $H_I$: $H_{II}$ in favor of the weakly bound hydrogen, which causes an increase in selectivity to olefins

## Author details

T. F. Sheshko and Yu. M. Serov
*Peoples' Friendship University of Russia, Russia*

## 5. References


[1] G. P. Van der Laan and A. A. C. M. Beenackers, 1999, "Kinetics and selectivity of the Fischer-Tropsch synthesis: a literature review," Catalysis Reviews, vol. 41, no. 3-4, pp. 255–318.

[2] Lapidus A.L., Krylova A.J., 2000, "The mechanism of formation of liquid hydrocarbons from CO and $H_2$ on cobalt catalysts ", Russian chemical journal, vol. XLIV, no. 1, pp. 4–18. [in Russian].

[3] Qinghong Zhang, Jincan Kang, Ye Wang. 2010, "Development of Novel Catalysts for Fischer–Tropsch Synthesis: Tuning the Product Selectivity. Review". vol. 2, no. 9, pp. 1030–1058.

[4] Tomoyuki T., Inui T. 1991 "Effective conversion of carbon dioxid." Catal. Today.. vol.10. no 1. pp.95-106

[5] Suzuki T., Mayama Y., Nayashi S. 1991. "Hydrogenation of carbon dioxide over iron catalyst". Kinet and Katal Lett. vol. 44. no 2. pp. 78-93

[6] Serov Yu. M., 1999. "Composite membranes for hydrogen recovery from gas mixtures, catalytic systems for vapor and carbon dioxide conversion of methane, detoxification of exhaust gases and the hydrogenation of carbon oxides ". Extended Abstract of Doctoral Dissertation in Chemistry (RUDN, Moscow, 1999). *[in Russian].*

[7] G. Erlich, Catalysis. Physical Chemistry of Heterogeneous Catalysis (Mir, Moscow, 1967) [in Russian].

[8] Wedler, G., Colb, K. G., Heinrich, W., McElhiney, G., "The interaction of hydrogen and carbon monoxide on polycrystalline iron films", Applications of Surf. Sci., 2(1), 1978, pp. 85-101.

[9] Sheshko T.F., Serov Yu. M., 2011 «Interaction of Carbon Oxides with the Surface of Catalysts Containing Iron and Nickel Nanoparticles» J. Russ.Phys. Chem. A 85, pp778-783.

[10] Popova N. M., Babenkova L. V. and Savel'eva G. A., 1985 "Application of Thermodesorption. Method to Adsorption and Catalysis (Nauka, Alma_Ata,) [in Russian].

[11] Mikhalenko I. I. and Yagodovskii V. D., Zh. Fiz. Khim. 79, 1540 (2005) [Russ. J. Phys. Chem. A 79, 1363(2005)].

[12] Edussuriya M. 1993 "Adsorption and hydrogenation of CO on powders of iron and ruthenium" (RUDN, Moscow, 1993). P. 153 [in Russian].

[13] Popova N.M., Babenkova L.V., Saveliev G.A. 1979. "Adsorption and interaction of simple gases with metals of Group VIII" . Alma-Ata: Nauka, 1979. P.278.

[14] Sokolova N.P. 1993 Russ. J. Phys. Chem. A 67, 10(1993).

[15] Tananaev I.V., Fedorov I.B., Kalashnikov E.G. 1987 "Progress of physical chemistry energy-environments". Successes of chemistry. 1987. T.56, N2. P.193.

[16] Mochoki A. 1991. "Fotmation of carbonaceous deposit and its effect of carbon monoxide hydrogenation on iron-based catalyst". Appl. Catal.. vol.70. no.2. pp. 253-267

[17] Rabo J.A., Risck A.P., Poutsma M.L 1978. "Reactions of carbon monoxide and hydrogen on Co,Ni,Ru and Pd metals". J. Catal. vol.53. pp.295-311.

[18] Catalysis in C1-chemistry. 1983. Edited by KEIM W. Institut fur Technische Chemie und Petrolchemie., D. Reidel Publishing Co., Dordrecht, Holland, 1983. 296p

[19] Gordon D., Watherbey C., Calvin H.B. 1987. "Hydrogenation of $CO_2$ on Group VIII Metals". J. Catal. vol.77. pp.82-91.

[20] Babenkova L V, Popova N M, Blagoveshchenskaya I N, 1985 "The Mechanism of the Reaction of Hydrogen with the Metals of the Iron Sub-group", Russ. Chem. Rev., vol.54. no2, pp. 105–116.

[21] Wenter J., Kaminsky M., Geoffroy G.L., Vannice M.A. 1987. "Carbon-supported Fe-Mn and K-Fe-Mn clusters for the synthesis of C2-C4 olefins from CO and $H_2$. Activity and selectivity maintenance and regenerability". J. Catal. vol. 105. pp.155-160.

[22] Andrew Campos, Nattaporn Lohitharn, Amitava Roy, Edgar Lotero, James G. Goodwin Jr., James J. Spivey 2010, "An activity and XANES study of Mn-promoted, Fe-based Fischer–Tropsch catalysts". Appl. Catal. A: General, Vol.375, pp. 12-16

[23] F. Morales, E. de Smit, F. M. F. de Groot, T. Visser, B. M. Weckhuysen. 2007. "Effects of manganese oxide promoter on the CO and $H_2$ adsorption properties of titania-supported cobalt Fischer–Tropsch catalysts". J.Catal. № 246, pp.91 –99.

[24] Slivinskii EV, Kliger, EA, L. Kuzmin, Abramov AV, Kulikov EA 2003, "Strategy for sustainable use of natural gas and other carbon compounds in the production of synthetic liquid fuels and petrochemical intermediates." Journal of Russ. Chem. Society nam. D.I. Mendeleev. . T. XLVII, № 6, pp.14-20. *[in Russian].*

[25] Sheshko T.F., Serov Yu.M., 2011, "Interaction of Carbon Oxides with the Surface of Catalysts Containing Iron and Nickel Nanoparticles". Russian Journal of Physical Chemistry, Vol. 85, no. 5, pp. 867–873.

[26] Ismailov, M.A., Akhverdiev R.B., Haji-Kasumov V.S., Matyshak V.A. 1992. "The structure and reactivity of surface complexes formed in the oxidation of CO with oxygen and NO on catalysts based on activated $Al_2O_3$". Kinetics and Catalysis. T.33, № 3, pp.611-617. *[in Russian].*

[27] Firsov A.A., Khomenko T.I., Silchenkova O.N., Korchak V.N. 2010. "The oxidation of CO in the presence of hydrogen in the oxides CuO, CoO and $Fe_2O_3$, deposited on $ZrO_2$". Kinetics and Catalysis. T.51. Number 2. pp.317-329.

[28] Nieuwenhuys B.E. 1983 « Adsorption and Reaction of CO, NO, $H_2$ and $O_2$ on Group YIII Metal Surface ». Surf. Sc. V.126, N1-3. pp.307-337.

[29] Levshin N.L. 2000. "The influence of adsorption-desorption processes on phase transitions in solids," Doctoral Dissertation in. phys. and Math., Moscow: Moscow State University.

[30] Matyshak V.A., Korchak V.N., Burdeinaya T.N., Tret'yakov V.F., Zakirova A.G., Lermontov A.S., Lunin V.V. 2008 "The mechanism of selective $NO_X$ reduction by hydrocarbons in excess oxygen on oxide catalysts: VII. The nature of synergism on a mechanical mixture of catalysts". Kinetics and Catalysis. 2008. V. 49. № 3. - pp. 413-420.

[31] Matyshak V.A., Ismailov I.T., Tretyakov V.F., Silchenkova O.N. 2011. " On the mechanism of conversion of ethanol to copper oxide catalysts for According to IR-spectroscopy *in sit* ". Russian Congress on Catalysis "RussCatalysis" 3 - 7 October, Moscow. Abstracts. V.II, p. 61

IntechOpen

IntechOpen